

Laser Ablation of Imidazolium Based Ionic Liquids[†]

Yury Dessiaterik, Tomas Baer,* and Roger E. Miller

Department of Chemistry, University of North Carolina, Chapel Hill, North Carolina 27599-3290

Received: June 14, 2005; In Final Form: July 14, 2005

Time-of-flight mass spectrometry has been used to investigate the IR ablation of several ionic liquid imidazolium salts of the form $R_1R_2\text{Iium X}$ (R_1 = methyl; R_2 = methyl, ethyl, butyl, and hexyl; X = Cl^- , NO_3^- , and CH_3SO_4^-). The ablated ionic species were analyzed by time-of-flight mass spectrometry using pulsed extraction, and neutral species were detected using vacuum UV photoionization at 10.5 eV. The results demonstrate that at least 99% of the ablated material is removed in the form of nano- or microdroplets consisting of intact ionic liquid. Approximately 1% is ejected as imidazole molecules ($R_1R_2\text{Im}$) produced through the elimination of HCl, and about 0.1% of the material is ejected in the form of single salt molecules of $R_1R_2\text{Iium X}$. A chemical thermometer was used to measure the internal temperature (475 ± 25 K) of the ablated vapor plume.

Introduction

Ionic liquids are a versatile class of low melting point organic salts that typically have no measurable vapor pressure at room temperature. They can be substituted for traditional organic solvents in a wide range of studies.^{1,2} In particular, they are used increasingly as solvents and catalysts in a wide range of organic syntheses.^{3–13} Ionic liquids have also been used as matrixes in matrix-assisted laser desorption/ionization (MALDI) time-of-flight mass spectrometry because of their excellent vacuum stability and their ability to dissolve polar and nonpolar solutes, including biological oligomers and proteins.¹⁴ Their effectiveness in this area is attributed to the fact that they are liquids, resulting in more homogeneous solutions for MALDI studies than their solid matrix counterparts.

A particularly interesting class of ionic liquids consists of imidazoles and triazoles, where the presence of two or three nitrogen atoms makes them rather unstable and the corresponding decomposition very exothermic. It is thus of interest to study their thermal decomposition kinetics and pathways. Several experimental studies of imidazolium salt pyrolyses have already been reported.^{15,16} In particular, systematic studies have been carried out on the pyrolysis of 1,3-dialkyl substituted imidazolium iodide salts¹⁵ with R_1 being methyl, ethyl, propyl, and butyl and R_2 as methyl, ethyl, propyl, butyl, benzyl, vinyl phenyl, and allyl. The effects of varying the anions, namely, I^- , Cl^- , Br^- , I^- , Ph_4B^- , and ClO^- in 1-ethyl-3-methylimidazolium were also investigated. Samples were heated to temperatures between 220 and 260 °C for 0.5–1.5 h, corresponding to pressures less than 2 Torr. The major degradation products for these salts were found to be neutral mono-N-alkylated imidazoles: R_1 -imidazole and R_3 -imidazole. The decomposition of ethylmethylimidazolium salts, with three different anions (Br, bis(trifluoromethanesulfonyl)amide, and bis(methanesulfonyl)amide), were recently studied by Baranyai et al.,¹⁶ who also found that the major cation degradants were neutral mono-N-alkylated imidazoles. They found that at temperatures as high as 300 °C, with heating times of 1 h, only 1% of the samples were decomposed, indicative of the high stability of this compounds.

Awad et al.¹⁷ recently reported the thermal desorption mass spectra for 1-decyl-1,2-dimethylimidazolium tetrafluoroborate. In this study, the sample was heated to between 400 and 550 °C, while electron impact ionization mass spectrometry was used to sample the resulting vapor. The thermal desorption spectra showed two maxima in the total ion signal, at 2.6 and 3.35 min, corresponding to a lower temperature degradation product resulting from the loss of a methyl group and a higher temperature product associated with H loss.

The decomposition of a variety of ionic liquids has also been studied using the method of acoustic cavitation,¹⁸ in which sonication results in the creation of bubbles in the liquid with local temperatures as high as 5000 K.¹⁹ The gases evolving from this process were then analyzed by GC–MS. Among the liquids studied were decylmethylimidazolium tetraphenylborate, butylmethylimidazolium chloride, butylmethylimidazolium tetrafluoroborate, and butylmethylimidazolium hexafluorophosphate. The major gaseous products in the decomposition of butylmethylimidazolium chloride were chlorobutane and chloromethane, and the products for the borate and phosphate liquids were 2-methylpropane and acetonitrile. On the basis of these studies, we conclude that slow heating of disubstituted imidazolium salts results in the formation of monosubstituted imidazole, whereas faster heating to higher temperatures results in the loss of an alkyl group or H atoms. In contrast, sonication results in ring opening reactions.

In light of the dependence of this degradation processes on the heating rate, it is interesting to consider the decomposition of ionic liquids upon laser ablation, where the heating rates are typically much faster than those discussed above. Previous laser ablation studies carried out in our laboratory have been based upon the use of aerosol samples, with an infrared laser (either CO_2 or Nd:YAG pumped OPO) timed to irradiate a particle as it passes through the ionization region of a time-of-flight mass spectrometer.²⁰ In the present study, a film of ionic liquid is placed directly in the mass spectrometer and the laser is focused onto the liquid. The initial gas-phase products are identified using single photon VUV ionization and time-of-flight mass spectrometry. Single photon photoionization greatly reduces fragmentation, compared to electron impact ionization or

[†] Part of the special issue "William Hase Festschrift".

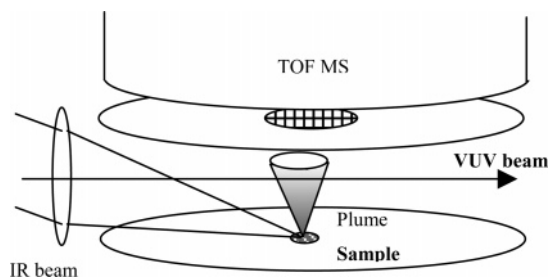


Figure 1. Experimental setup in which the IR laser beam is focused by a 25 cm NaCl lens onto the liquid salt sample. The vacuum UV (VUV) laser was fired after some delay relative to the IR laser pulse. Ions were mass analyzed by time-of-flight (TOF).

multiphoton ionization with UV lasers.^{21–23} The temperature of the ablated salt was monitored by adding a “thermometer molecule” (ethylene glycol) to the ionic liquid. This measurement is based upon the fact that the internal energy dependence of the fragmentation pattern of ethylene glycol ion is well-known.²⁴

Experimental Setup

The experimental setup used in the present study is shown in Figure 1. A pipet was used to place approximately 100 mg of the ionic liquid on the ion repeller plate of a time-of-flight (TOF) mass spectrometer. Two IR lasers were used to ablate the sample, namely a pulsed CO₂ laser (Lumonics) with pulse energies as high as 500 mJ and a tunable OPO laser (Laser Vision) pumped by a Nd:YAG laser (Continuum) that generated a pulse energy of 10 mJ. The OPO laser wavelengths were chosen to match the absorption peak of CH stretches of the ionic liquid around 2950 cm⁻¹.

The ablation lasers were focused on the sample by a 25 cm focal length NaCl lens, and the ablated ions were pulse extracted from the ionization region at variable delays, between 1 and 100 μs. The voltages in the first and second extraction fields were chosen to space-focus²⁵ ions in the middle of the ionization source (10 mm from both the extraction and repeller plates). When the delay between the ablation laser and pulse extraction field was small (less than 5 μs), the pulsed extraction occurred before the ablated ions could reach the midpoint between the two plates. As a result, their TOF was shifted to shorter times, relative to the ions that started from the space focusing point, because they gained more energy in the acceleration region and thus moved more quickly through the 1 m drift region. However, as the time delay for pulsed extraction increased, the ions had more time to drift to the “sweet spot” so that the TOF shifted to the correct value. In the other extreme, the ablated ions moved through the first acceleration region before the extraction pulse was applied, resulting in very broad TOF peaks.

The neutral products resulting from laser ablation were studied by ionizing them with a vacuum UV laser pulse at 10.5 eV. The 118.5 nm (10.5 eV) VUV laser light was produced by frequency tripling the 355 nm output of a Nd:YAG laser (Continuum) in a mixture of Xe and Ar gas, as described in detail elsewhere.²⁴ The VUV laser was loosely focused to a spot of 1 mm² in the midpoint of the ionization region of the

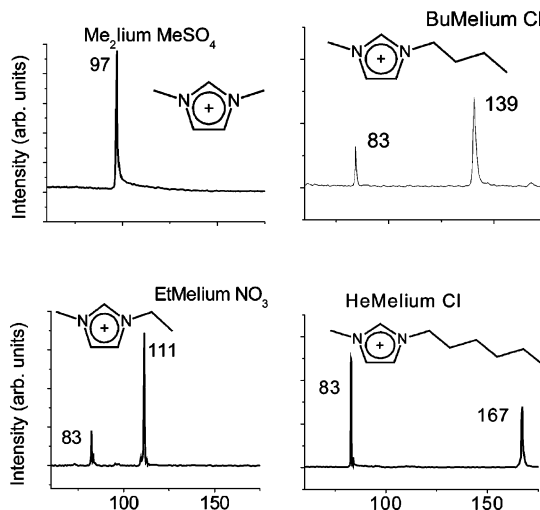
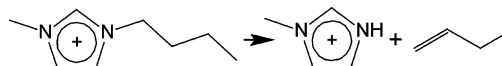


Figure 2. Positive ion mass spectra of ionic liquid salts using only the CO₂ laser. In each case the high mass peak corresponds to the salt cation that has lost its negative ion.

SCHEME 1: Decomposition Pathway for Imidazolium Ions with BuMeIium as an Example



TOF mass spectrometer. The time delay between the IR and VUV laser was varied from 15 to 100 μs. The pulsed extraction was typically initiated a few hundred nanoseconds after the VUV laser was fired. In some experiments, where the delay between the IR and VUV laser was short, a voltage of -50 V was applied to the repeller to remove ablated ions before the VUV laser was fired.

Table 1 lists the ionic liquids that were used in the present study, all of which were obtained from Sigma Aldrich and used without purification. Choice of the anionic part of the salts was dictated by their availability from the supplier.

Results and Discussion

Mass Spectra from IR Laser Ablation. Figure 2 shows a series of mass spectra corresponding to four ionic liquid samples irradiated with the CO₂ laser at fluences between 0.9 and 10 J/cm². The major peaks for these R₁R₂Iium X compounds correspond to the R₁R₂Iium⁺ cations and fragment ions formed by breaking the N–C bond, accompanied by a hydrogen atom transfer to the nitrogen group (Scheme 1). The resulting fragment ion, formed by unimolecular decomposition of the R₁R₂Iium⁺ cation, therefore appears in each case at an *m/z* of 83. In the case of Me₂Iium X, only the Me₂Iium⁺ ion is observed, presumably because there was insufficient energy to break the N–C bond to the methyl group and the hydrogen transfer would produce the unstable CH₂ neutral fragment. It is also confirmed by the fact that ions with loss of CH₂ were not detected for other ionic liquids. The four spectra in Figure 2 were obtained with about the same CO₂ laser fluence of 350 mJ/pulse. It is evident that the ratio of the mass 83 to parent ion increases as

TABLE 1

ionic liquid	MW	MP, °C
1,3-dimethylimidazolium methyl sulfate (Me ₂ Iium MeSO ₄)	208.24	<20
1-ethyl-3-methylimidazolium chloride (EtMeIium Cl)	146.62	77–79
1-ethyl-3-methylimidazolium nitrate (EtMeIium NO ₃)	173.17	38–41
1-butyl-3-methylimidazolium chloride (BuMeIium Cl)	174.67	55
1-hexyl-3-methylimidazolium chloride (HeMeIium Cl)	202.72	-85

the R group gets bigger. This is probably related to the increased stability of the larger neutral leaving group, which reduces the activation energy for m/z 83 ion formation.

On the basis of the signal level, we have estimated that about 10^6 ions are detected per laser shot.

Negative ion mass spectra were also recorded under these ablation conditions. For the two ionic liquids containing chloride, the Cl^- ion peak was very strong. The major impurity peaks were assigned to CN^- (m/z 26) and FeCl_3^- [m/z 161, 163, 165]. The latter species were most likely the result of the laser hitting the stainless steel plate onto which the ionic liquid was placed. In the case of EtMeIium NO_3 , the negative ion spectra showed NO_2^- , NO_3^- peaks, and impurities that were assigned as CN^- , NCO^- , and tentatively HNO_4^- (at mass 79).

Mass spectra obtained using the OPO laser were qualitatively similar to those obtained with the CO_2 laser. The OPO laser wavelength was set to 2950 cm^{-1} , corresponding to the absorption maximum in the C–H stretch region. The pulse duration was approximately 5 ns, and the pulse energy was in the range 1–8 mJ/pulse. A laser spot size of $120 \times 400\ \mu\text{m}$ was measured by collecting burn spots on thermal paper and scanning them with a resolution 600 dpi. The absorption length (λ) in the ionic liquid, which is a measure of the laser beam transmittance, was measured to be about $37\ \mu\text{m}$ for HeMeIium Cl, by placing a sample of the liquid between two BaF_2 windows, spaced by $100\ \mu\text{m}$, and measuring the intensities of the incident (I_0) and transmitted (I) light. Beer's law was then used to determine λ , where d is the sample thickness:

$$I = I_0 \cdot \exp\left(-\frac{d}{\lambda}\right) \quad (1)$$

As noted above, the mass spectra resulting from ablation of HeMeIium Cl, EtMeIium Cl, and EtMeIium NO_3 using the OPO and CO_2 lasers were qualitatively the same. However, larger pulse energies (20–400 mJ) were required with the CO_2 laser to obtain the same signal level. This difference is in part a result of the longer absorption length at the CO_2 laser wavelength (150 μm), compared to $37\ \mu\text{m}$ at the OPO laser wavelength of 2950 cm^{-1} . In addition, the temporal profile of the CO_2 laser is quite different, consisting of an initial 300 ns spike, and an exponential tail with a 1.2 μs time constant. As a result, the ion signal obtained for HeMeIium Cl with a CO_2 laser pulse energy of 160 mJ was approximately the same as that obtained from the OPO laser pulse at an energy of 8 mJ/pulse. After the difference in the absorption lengths at the two wavelengths is corrected for, the OPO laser is still 5 times more efficient in ablating the ionic liquid, a result of its higher peak power. However, this difference is not easily accounted for quantitatively, given that the two lasers are so different in their pulse width and spot size. The influence of laser fluence (J/m^2) and laser spot size have been extensively studied both experimentally,²⁶ and by molecular dynamics simulations.²⁷ The shorter pulse width of the OPO laser clearly enhances ablation, whereas the smaller spot size makes it less efficient compared to the CO_2 laser, presumably because energy loss by conduction is more important in smaller spot sizes.

The velocity of the HeMeIium⁺ ions was measured using a zero-field technique, in which the ions were allowed to traverse the first acceleration region while both electrodes were grounded. The time that the ions needed to cross this region was measured by the application of an extraction pulse at various delay times after the IR laser pulse. The measured velocity of the ion was found to be about 4 times that of the neutrals. Before we attribute the observed ion velocities to a specific ablation mechanism, it

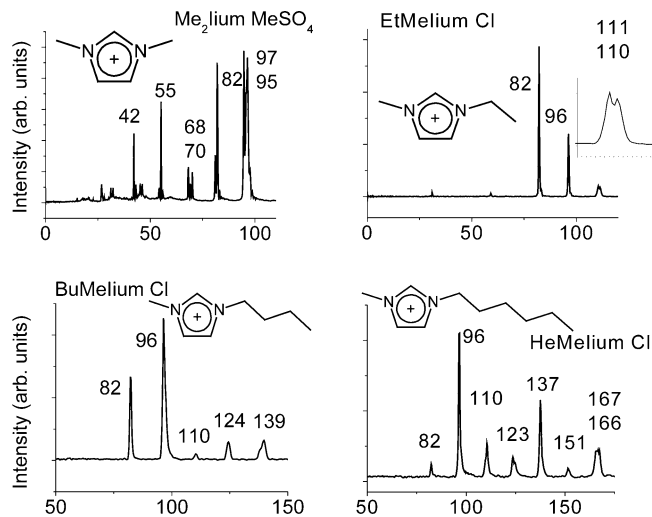
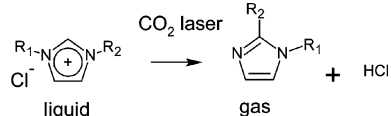
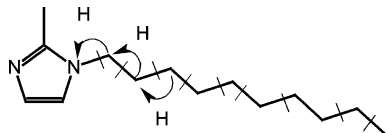


Figure 3. Mass spectra of neutrals obtained by VUV laser postionization of IR laser ablation plume.

is worth considering the findings of Gluckmann et al.,²⁸ who concluded that zero-field measurements can be strongly affected by penetration of the dc acceleration field (from the second acceleration stage) into the nominally zero-field first stage. To estimate this fringing field, we carried out a numerical simulation for the wire mesh geometry used here. La Place's equation for the electric potential was solved using a finite elements partial differential equation solver.²⁹ The equation was solved in two dimensions (cylindrical symmetry) with the symmetry axes going through the center of the mesh cell. The result of the simulation suggests that, for the present configuration (20 mm spacing between the ion extraction plates, a 5 mm second acceleration field of 5300 V/m, and a 70 lines/in. 90% transparency grid between these two fields), ions in the center of the ionization region can be accelerated by as much as 11 eV due to field penetration, providing an adequate explanation for the experimental data. Thus, the high velocity of the ions from the ablation plume, relative to the neutral species, is an artifact of the experimental technique and is not a characteristic of the ablation process.

Detection of Neutral Ablation Products. Figure 3 shows a series of mass spectra recorded using the VUV laser to ionize the neutrals ablated by the IR laser. Care was taken to ensure that directly produced ions did not contribute to the VUV laser induced mass spectra. These mass spectra are much richer than those corresponding to the ions produced directly by the infrared laser. In all cases, the $\text{R}_1\text{R}_2\text{Iium}^+$ cation peak is observed, suggesting that intact ionic salt molecules, $\text{R}_1\text{R}_2\text{Iium X}$, are ejected in the ablation process and photoionized to yield the ion pair, $\text{R}_1\text{R}_2\text{Iium}^+ + \text{X}^-$. However, close examination of these peaks, for the cases of BuMeIium Cl and HeMeIium Cl, shows that they are doublets separated by one mass unit. This lower mass peak corresponds to the imidazolium salt that has lost HCl. Evidence provided later indicates that this ablation product is a neutral imidazole molecule, which is produced by the migration of the R₁ group from the nitrogen to the carbon atom, as shown in Scheme 2. Similar HCl (or HX) loss reactions have been reported in the high temperature thermal desorption mass spectrometry.^{17,30}

The remaining peaks in the mass spectra of EtMeIium, BuMeIium, and HeMeIium salts are associated with the loss of methyl, ethyl, propyl, etc. groups from the R₁ side chain of the imidazole molecule, as shown in Scheme 3. In the case of Me₂Iium MeSO₄ we see evidence for ring opening, a process

SCHEME 2: Decomposition Pathway for Imidazolium Salt Molecule**SCHEME 3: HeMeIium Cl Decomposition Pathway**

that seems to be absent in the other molecules. This difference is readily accounted for by the relative energetics associated with fragmenting the side chain and ring opening processes. The former certainly requires less energy so that the rate of side chain fragmentation is higher than ring opening. As a result, the ion preferentially dissociates by side chain fragmentation when this route is available. In the case of the dimethyl compound, side chain fragmentation is not possible so that ring opening is observed

There are two possible routes for production of the lower mass fragment ions seen in these mass spectra. First, the IR laser could impart sufficient energy to fragment the neutral molecule, as in Scheme 3, with the VUV laser simply ionizing these fragments. Alternatively, the IR laser might only produce the imidazole molecule, as in Scheme 2, whereas the VUV laser dissociatively ionizes this molecule. In general, the latter mechanism is more likely given that ions tend to fragment more easily than their neutral closed shell counterparts.

The first evidence in support of the dissociative photoionization is contained in the mass spectrum itself. If the IR laser produced the various fragments in Scheme 3, we would expect to see not only the higher mass peaks but also their complementary mass peaks. For instance, the complementary fragment associated with m/z 96 would be a pentene (C_5H_{10} , m/z 70), which has an ionization energy of 9.5 eV³¹ and would thus be readily ionized by the VUV laser. These low mass ions are not observed in the HeMeIium Cl mass spectrum in Figure 3. Similarly, in the mass spectrum for EtMeIium Cl, the complementary fragment of the m/z 82 peak would be C_2H_4 (ionization energy of 10.51 eV³¹), which should also be observed by VUV ionization. Here again, we see no evidence for a peak at m/z 28 in Figure 3. We thus conclude that the VUV generated fragment ions were formed by dissociative photoionization of vibrationally excited neutral imidazole. Apparently the IR ablation does not result in significant fragmentation of the alkyl chain.

Neutral Molecule Velocity Distributions. Further evidence for dissociative photoionization can be obtained from the neutral molecule velocity distributions, which were determined by measuring the intensity of the photoionization signal as a function of the time delay between OPO and VUV laser pulses. Figure 4 shows the dependence of the ion signals on the time delay for the various peaks in the HeMeIium Cl mass spectrum. The experimental data were fit to the equation suggested by Wedler and Ruhmann,^{32,33} namely $P(t) \sim 1/t^4 \exp(-t_0^2/t^2)$, where t_0 corresponds to the time of maximum flux. The maxima in the arrival time distributions occur at $24.6 \pm 3 \mu s$ for the lower mass ions and $30.7 \mu s$ for the m/z 166/167 parent ions. With the exception of the parent ion (325 m/s), the most probable velocity for all the ions is 410 m/s. Given that the ions with masses from 96 to 151 all have the same velocity

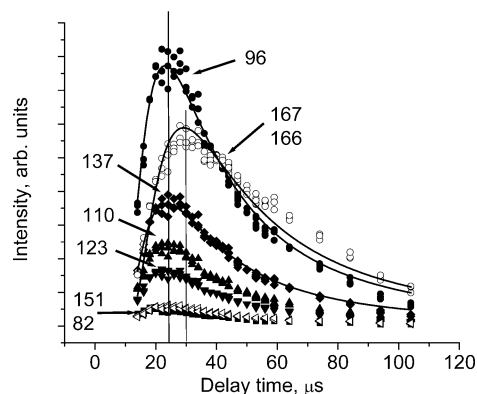


Figure 4. Ion signals vs time delay between the ablation and ionization lasers. Solid lines are fits using a Maxwell–Boltzmann distribution of velocities.

distribution, we concluded that they must have a common source. This conclusion is entirely consistent with the previous deduction that the IR ablation does not produce a large distribution of neutral products. It is most probable that the parent molecule that dissociatively ionizes to produce the observed fragments is the HCl loss product from HeMeIium Cl of mass 166. Unfortunately, the limited mass resolution prevented us from determining the velocity distribution for this species in the presence of the m/z 167 ion.

The neutral molecule that gives rise to mass peak 167 has a lower translational velocity and is most likely associated with the parent molecule (HeMeIium Cl) that loses Cl^- after photoionization. Its low translational energy suggests that it originated from a low temperature part of the ablation plume. Because the sample thickness is much greater than the penetration depth of the IR radiation, heating of the sample is likely to be nonuniform. The cooler portions of the ablation process will favor the formation of stable parent ions, and the hotter regions will result in vibrationally excited neutral species that dissociate upon photoionization.

There is an apparent contradiction in suggesting that the heating is nonuniform, while at the same time using a Maxwell–Boltzmann distribution to fit experimental data. However, as was pointed out by Zhigilei and Garrison,³⁴ a modified Maxwell–Boltzmann distribution can be used to obtain a satisfactory description of the experimental data, although the interpretation of the fitted parameters in terms of physical properties of the ejected plume is often problematic. In the present study, this distribution is simply used to compare the average translational energies of the fragments.

Imidazole Mass Spectrum. Further evidence in support of imidazole formation (Scheme 2) and its dissociative photoionization comes from comparing the results in Figure 3 with the mass spectrum obtained from the 1-decyl-2-methylimidazole molecule (DeMeIm). When room temperature DeMeIm vapor was photoionized, only the parent ion was observed in the mass spectrum. However, when the liquid sample was irradiated with the OPO laser prior to VUV photoionization, we obtained an ion fragmentation pattern (Figure 5) that is very similar to that obtained for the ionic liquids. Namely, it consists of the parent peak at m/z 222, followed by the loss of methyl (m/z 207), ethyl, and propyl radicals, consistent with simple C–C bond cleavage steps proposed for HeMeIium Cl. However, the lower mass fragment ions, associated with larger neutral fragments, switch over to rearrangement reactions resulting in the production of even m/z peaks, including 110 and 96, once again as observed in Figure 3.

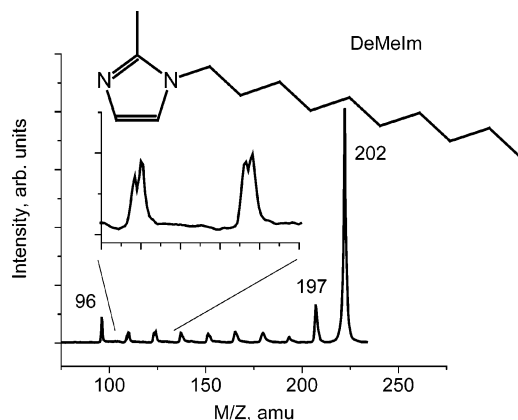


Figure 5. Photoionization mass spectra of 1-decyl-2-methylimidazole, after vaporization with the OPO IR laser.

The possible formation of hexyl chloride was excluded by collecting a photoionization mass spectrum of hexyl chloride vapor. The main peaks at masses 91 and 93 correspond to the loss of ethyl radical. The absence of these mass peaks in the photoionization spectrum of the HeMeIium Cl ionic liquid sample indicates that they were not produced in the ablation process.

Collecting Ablation Products and Formation of Nanodroplets. All of the experimental evidence suggests that the IR ablation process of imidazolium salts either vaporizes the intact liquid or results in the loss of HCl to form a neutral imidazole molecule. To confirm this and to quantify the ablation process, we collected ablation products from 36 000 OPO laser pulses (7 mJ/pulse) on a piece of aluminum foil. The foil was placed 12 mm from the sample, parallel to the extraction plates. The sample mass was measured before and after the experiment, as was the mass of the material deposited on the foil. In a typical experiment, we found that the mass lost from the sample was 37 mg, whereas the mass of the ablation product (deposited on the aluminum foil) was 35 mg, suggesting that more than 90% of material was collected.

The ablated material was dissolved in methanol and analyzed with positive ion electrospray mass spectrometry. We found that both the pure sample and the ablation product gave mass spectra characteristic of HeMeIium Cl, indicating that the ablation process does not result in massive decomposition of the ionic liquid. The collection of the ablation products enables us to estimate the amount of material removed from the target per laser shot. In particular, 35 mg of sample was ejected and deposited on the foil, on an approximately 1 cm diameter circular area. This corresponds to the removal of approximately 10^{15} molecules per laser shot, in agreement with the number of molecules in the laser spot area (5×10^{15} molecules in 0.04 mm^2). If we assume that the plume of ionic liquid generated by the IR laser irradiation is uniformly distributed inside a cone, with a 30° solid angle, the volume of this cone (up to the VUV laser irradiation point) is 0.1 cm^3 , yielding a molecular density of 10^{16} cm^{-3} .

This leads to the obvious question: how much of this is in the form of the ionic salt and how much is due to imidazole (having lost HCl)? The gas density of the ablated imidazole can be determined by comparing the VUV photoionization signal with that obtained from a known pressure of aniline vapor. Aniline vapor at a pressure of $4 \mu\text{Torr}$ (10^{11} molecules/ cm^3) yields a signal of $6 \times 10^{-4} \mu\text{V}$. Assuming a similar photoionization cross section for the ionic liquid, we estimate that the signal from HeMeIm (at a vapor density of 10^{16} cm^{-3}) would

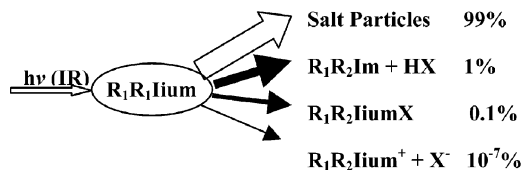


Figure 6. Branching ratios of products generated by IR laser ablation of imidazolium ionic liquids.

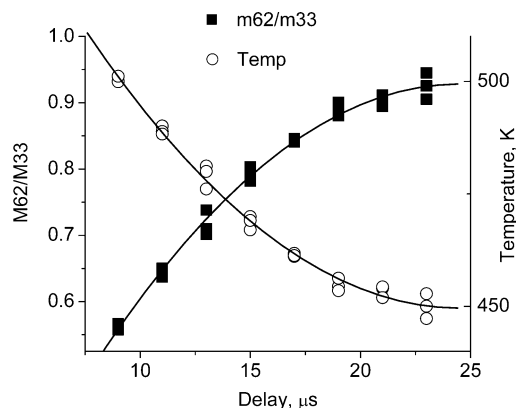


Figure 7. Determination of ablated ionic liquid temperature with ethylene glycol (EG) thermometer; the ratio of areas of parent ion signal to mass 33 signal vs delay between OPO and VUV lasers, OPO pulse energy 8.7 mJ.

be $60 \mu\text{V}$. However, the measured signal is only $0.3 \mu\text{V}$, which corresponds to a gas density of 5×10^{13} . The implication is that more than 99.5% of the ablated plume is not detected by the VUV laser. We propose that the plume consists predominantly of microdroplets, which are too heavy to be extracted by the TOF system. The ejection of such microdroplets has been observed previously in the laser ablation of aqueous media,³⁵ where the droplets were detected by flash photography. Computer simulations^{27,36} have also shown that a significant fraction of the ablated material is removed in the form of clusters. Thus, taken together, the mass balance and the ion signals lead us to the conclusion that IR laser ablation of the ionic salts leads to 99% removal of intact salt in the form of nano- or microdroplets and only 1% leads to the production of vapor, corresponding to HCl loss. The composition of the ablation plume is shown in Figure 6.

Internal Energy of Ablated Molecules. The internal energy of molecules in the plume was estimated using a chemical thermometer. This technique, described by Woods et al.,²⁴ involves measuring the mass spectrum as a function of temperature for a molecule whose corresponding fragmentation pattern is known. Such data are available for ethylene glycol,³⁷ which was added to the HeMeIium Cl sample (5 vol %). The measured ratio of parent ion ($\text{OHCH}_2\text{CH}_2\text{OH}^+$) and fragment ion (CH_3OH_2^+) peak areas are shown in Figure 7, as a function of VUV/OPO laser delay and the OPO laser power. On the basis of the previous temperature calibration,²⁴ we conclude that the temperature drops from 500 K to 450 K as the time delay increases from 10 to 25 μs . This temperature is close to that found in thermal gravimetric analysis (TGA) experiments, in which the imidazolium chloride salts decompose.³⁸

Parent Ion Signal. It is interesting to note that the parent ion ($\text{R}_1\text{R}_2\text{Iium}^+$) is not observed in the thermal decomposition of imidazolium salts.³⁹ In contrast, we detect the parent cation for all of the ionic liquids studied here. This is most likely the result of the much faster heating rates realized in the present laser ablation experiment. For thermally labile compounds, the rate of decomposition k_d at low temperature is higher than the

evaporation rate, k_v . However, from the isothermal decomposition rate of $\text{Me}_2\text{BuIium BF}_4^{38}$ we can estimate that the entropy change for the decomposition is negative. Because the entropy change for vaporization is positive, we expect that at sufficiently high temperatures the vaporization rate (k_v) will be higher than the rate of decomposition k_d . At the heating rates common for TGA experiments (ca. 10 K/s) the samples decompose before they evaporate. In contrast, in laser ablation experiment the heating rate can be as high as 10^8 – 10^{13} K/s.⁴⁰

We should note that the data shows that more decomposition occurs at higher OPO powers. Nevertheless, we do expect to vaporize more parent molecules at higher temperature. These results can be understood if we assume that the parent molecules continue to decompose after vaporization.

Conclusions

We have reported the results of a study of the IR laser ablation of ionic liquids, consisting of several alkyl substituted imidazolium salts. The major ablation product (99%) is found to be nano or microdroplets of the intact ionic salt. The remaining 1% is divided between the salt cation, $\text{R}_1\text{R}_2\text{Iium}^+$, gas-phase salt molecules ($\text{R}_1\text{R}_2\text{Iium X}$), and the alkyl substituted imidazole produced by the loss of HCl from the imidazolium salt. For IR laser ablation of $\text{Me}_2\text{Iium MeSO}_4$ only the parent cation (Me_2Iium^+) is observed. For all other imidazolium salts ($\text{R}_1\text{MeIium X}$) a second peak was detected at m/z 83, corresponding to R_2 radical loss. The neutral species ejected in the ablation plume were investigated by vacuum UV photoionization, with the laser being delayed by a few microseconds from the IR ablation laser. The neutral ablated species consist of the parent molecule ($\text{R}_1\text{MeIium X}$) and an imidazole molecule formed by the loss of HCl upon ionization.

It is particularly noteworthy that the major decomposition product from IR laser ablation corresponds to the loss of HCl, which is in contrast to the loss of R_1Cl , R_2Cl , found in the experiments at lower heating rates.^{15,16}

Acknowledgment. We thank the U.S. Air Force Office of Scientific research for a grant.

References and Notes

- (1) Tolley, L.; Jorgenson, J. W.; Moseley, M. A. *Anal. Chem.* **2001**, *73*, 2985–2991.
- (2) Sheldon, R. *Chem. Commun.* **2001**, 2399–2407.
- (3) Adams, C. J.; Earle, M. J.; Seddon, K. R. *Chem. Commun.* **1999**, *11*, 1043–1044.
- (4) Adams, C. J.; Earle, M. J.; Roberts, G.; Seddon, K. R. *Chem. Commun.* **1998**, 2097–2098.
- (5) Fischer, T.; Sethi, A.; Welton, T.; Woolf, J. *Tetrahedron Lett.* **1999**, *40*, 793–796.
- (6) Kitazume, T.; Kasai, K. *Green Chem.* **2001**, *3*, 30–32.
- (7) Earle, M. J.; McCormac, P. B.; Seddon, K. R. *Green Chem.* **1999**, *1*, 23–25.
- (8) Chiappe, C.; Capraro, D.; Conte, V.; Pieraccini, D. *Org. Lett.* **2001**, *3*, 1061–1063.
- (9) Carmichael, A. J.; Earle, M. J.; Holbrey, J. D.; McCormac, P. B.; Seddon, K. R. *Org. Lett.* **1999**, *1*.
- (10) Rodriguez, M.; Segal, A.; Taddei, M. *Org. Lett.* **2003**, *5*, 4029–4031.
- (11) Miao, W.; Chan, T. H. *Org. Lett.* **2003**, *5*, 5004–5005.
- (12) Jessop, P. G.; Stanley, R. R.; Brown, R. A.; Eckert, C. A.; Liotta, C. L.; Ngo, T. T.; Pollet, P. *Green Chem.* **2003**, *5*, 123–128.
- (13) Dullius, J. E. L.; Suarez, P. A. Z.; Einloft, S.; Souza, R. F.; Dupont, J.; Fischer, T.; Cian, D. *Organometallics* **1998**, *17*, 815–819.
- (14) Carda-Broch, S.; Berthod, A.; Armstrong, D. W. *Rapid Commun. Mass Spectrom.* **2003**, *17*, 553–560.
- (15) Chan, B. K. M.; Chang, N. H.; Grimmett, M. R. *Aust. J. Chem.* **1977**, *30*, 2005–2013.
- (16) Baranyai, K. J.; Deacon, G. B.; MacFarlane, D. R.; Pringle, J. M.; Scott, J. L. *Aust. J. Chem.* **2004**, *57*, 145–147.
- (17) Awad, W. H.; Gilman, J. W.; Nyden, M.; Harris, R. H.; Sutto, T. E.; Callahan, J.; Trulove, P. C.; DeLong, H. C.; Fox, D. M. *Thermochim. Acta* **2004**, *409*, 3–11.
- (18) Oxley, J. D.; Prozorov, T.; Suslick, K. S. *J. Am. Chem. Soc.* **2003**, *125*, 11138–11139.
- (19) McNamara, W. B.; Didenko, Y. T.; Suslick, K. S. *Nature* **1999**, *401*, 772–775.
- (20) Dessiaterik, Y.; Nguyen, T. G.; Miller, R. E.; Baer, T. *J. Phys. Chem. A* **2003**, *107*, 11249–11256.
- (21) Arps, J. H.; Chen, C. H.; McCann, M. P.; Datskou, I. *Appl. Spectrosc.* **2001**, *43*, 1211–1214.
- (22) van Bramer, S. E.; Johnston, M. V. *J. Am. Soc. Mass Spectrom.* **1989**, *1*, 419–426.
- (23) van Bramer, S. E.; Johnston, M. V. *Appl. Spectrosc.* **1991**, *46*, 255–261.
- (24) Woods, E., III; Miller, R. E.; Baer, T. *J. Phys. Chem. A* **2003**, *107*, 2119–2125.
- (25) Wiley, W. C.; McLaren, I. H. *Rev. Sci. Instrum.* **1955**, *26*, 1150–1157.
- (26) Dreisewerd, K.; Schurenberg, M.; Karas, M.; Hillenkamp, F. *Int. J. Mass Spectrom. Ion. Processes* **1995**, *141*, 127–148.
- (27) Zhigilei, L. V.; Garrison, B. J. *Appl. Phys. Lett.* **1999**, *74*, 1341–1343.
- (28) Gluckmann, M.; Karas, M. *J. Mass Spectrom.* **1999**, *34*, 467–477.
- (29) FlexPDE4. [4.2.12s]. 3–30–2005. PDE Solutions Inc.
- (30) Moens, L.; Blake, D. M.; Rudnicki, D. L.; Hale, M. J. *J. Solar Energy Eng.* **2003**, *125*, 112–116.
- (31) Lias, S. G. *NIST Chemistry WebBook: NIST Standard Reference Databas 69*; Nat. Inst. Standards and Tech/http://webbook.nist.gov: Gaithersburg, MD 20899, 2003.
- (32) Wedler, G.; Ruhmann, H. *Surf. Sci.* **1982**, *121*, 464–486.
- (33) Kelly, R.; Dreyfus, R. W. *Surf. Sci.* **1988**, *198*, 263–276.
- (34) Zhigilei, L. V.; Garrison, B. J. *Appl. Phys. Lett.* **1997**, *72*, 551–553.
- (35) Oraevsky, A. A.; Jacques, S. L.; Tittel, F. K. *J. Appl. Phys.* **1995**, *78*, 1281–1290.
- (36) Zhigilei, L. V.; Kodali, P. B. S.; Garrison, B. J. *J. Phys. Chem. B* **1997**, *101*, 2028–2037.
- (37) Li, Y.; Baer, T. *J. Phys. Chem. A* **2002**, *106*, 8658–8666.
- (38) Fox, D. M.; Gilman, J. W.; De Long, H. C.; Trulove, P. C. 206th Meeting of The Electrochemical Society, Honolulu, HI, 2004.
- (39) Abdul-Sada, A. K.; Greenway, A. M.; Seddon, K. R.; Welton, T. *Org. Mass Spectrom.* **1993**, *28*, 759–765.
- (40) Levis, R. J. *Annu. Rev. Phys. Chem.* **1994**, *45*, 483–518.